Biological impact of advanced glycation endproducts on estrogen receptor-positive MCF-7 breast cancer cells

Sabine Matou-Nasri[a,*,1], Hana Sharaf[c,1], Qiuyu Wang[c], Nasser Almobadel[a], Zaki Rabhan[a], Hamad Al-Eidi[a], Wesam Bin Yahya[a], Thadeo Trivilegio[b], Rizwan Ali[b], Nasser Al-Shanti[c], Nessar Ahmed[c,*]

[a] Cell and Gene Therapy Group, Medical Genomics Research Department, King Abdullah International Medical Research Centre, Ministry of National Guard Health Affairs, Riyadh 11426, Saudi Arabia
[b] Core Facility, King Abdullah International Medical Research Centre, Ministry of National Guard Health Affairs, Riyadh 11426, Saudi Arabia
[c] School of Healthcare Science, Manchester Metropolitan University, Manchester, M1 5GD, United Kingdom.

A R T I C L E   I N F O

A B S T R A C T

Diabetes mellitus potentiates the risk of breast cancer. We have previously described the pro-tumorigenic effects of advanced glycation endproducts (AGEs) on estrogen receptor (ER)-negative MDA-MB-231 breast cancer cell line mediated through the receptor for AGEs (RAGE). However, a predominant association between women with ER-positive breast cancer and type 2 diabetes mellitus has been reported. Therefore, we have investigated the biological impact of AGEs on ER-positive human breast cancer cell line MCF-7 using in vitro cell-based assays including cell count, migration, and invasion assays. Western blot, FACS analyses and quantitative real time-PCR were also performed. We found that AGEs at 50–100 μg/mL increased MCF-7 cell proliferation and cell migration associated with an enhancement of pro-matrix metalloproteinase (MMP)-9 activity, without affecting their poor invasiveness. However, 200 μg/mL AGEs inhibited MCF-7 cell proliferation through induction of apoptosis indicated by caspase-3 cleavage detected using Western blotting. A phospho-protein array analysis revealed that AGEs mainly induce the phosphorylation of extracellular-signal regulated kinase (ERK)1/2 and cAMP response element binding protein-1 (CREB1), both signaling molecules considered as key regulators of AGEs pro-tumorigenic effects. We also showed that AGEs up-regulate RAGE and ER expression at the protein and transcript levels in MCF-7 cells, in a RAGE-dependent manner after blockade of AGEs/RAGE interaction using neutralizing anti-RAGE antibody. Throughout the study, BSA had no effect on cellular processes. These findings pave the way for future studies investigating whether the exposure of AGEs-treated ER-positive breast cancer cells to estrogen could lead to a potentiation of breast cancer development and progression.

1. Introduction

Diabetes mellitus is a major public health concern with an increasing high prevalence and incidence that represents the seventh leading cause of death in the US, European nations and developed countries [1–3]. Type 2 diabetes mellitus is the most common form and a long-term chronic metabolic disorder characterized by hyperglycemia, mainly due to untreated insulin resistance [4]. During hyperglycemia, increased glycation of macromolecules (proteins, lipids or nucleic acids) occurs and leads to the formation of so called advanced glycation endproducts (AGEs) [5]. These AGEs are complex, fluorescent and crosslinked molecules of pathological significance [6]. Although this hyperglycemia-induced glycation is a non-specific reaction,

proteins undergo this modification more frequently than other macromolecules, with substantial functional and structural consequences [7–11]. Different clinical studies have reported the role of AGEs in the pathogenesis of various types of cancers in patients with diabetes mellitus, including colorectal [12], kidney [13], and liver cancer [14]. Lately, a growing body of evidence has suggested the direct consequences of diabetes-related hyperglycemia and hyperinsulinemia as AGEs can increase the development and progression of breast cancer [15–17].

Breast cancer is the second common cause of death with the highest incidence in women worldwide. This heterogeneous malignancy is characterized by a high diversity of morphological, molecular and biochemical features influencing disease progression, prognosis and

response to therapy [18]. Breast cancer subtypes are classified based on whether they are hormone- or non-hormone-dependent and referred for instance as estrogen receptor (ER)-positive or ER-negative, respectively. Of note, about 70% of breast cancer cases are ERα-positive [19]. Moreover, a growing body of evidence show that aerobic tumor cells are largely dependent on glycolysis, rather than oxidative phosphorylation, for their energy supply, a phenomenon known as the Warburg effect [20]. This altered energy metabolism generates cytotoxic sugar-derived reactive carbonyl compounds such as methylglyoxal, which promotes AGE formation in cancer cells [21]. Marked increases in the methylglyoxal and AGEs generated have been detected and correlated with breast cancer progression [22].

The cellular effects of AGEs are mainly mediated through the receptor for AGEs (RAGE) [23]. Highly expressed during embryonic development, RAGE expression level is low in the majority of healthy adult tissues while its expression is induced in pathological conditions (i.e. hyperglycemia, oxidative stress, hypoxia, inflammation) [24–26]. AGEs-RAGE interaction leads to the activation of signaling pathways (e.g., extracellular-signal regulated kinase [ERK]1/2, protein kinase C, cAMP response element binding protein-1 [CREB1], phosphoinositol-3 kinase [PI-3K], nuclear factor [NF]-κB phosphorylation) resulting in the production of inflammatory mediators that stimulate various cellular functions capable of promoting cancer [23,27]. We previously showed that methylglyoxal-derived bovine serum albumin AGEs (MG-BSA-AGEs) increased the proliferation, migration and invasion of ER-negative MDA-MB-231 breast cancer cell line, in a RAGE-dependent manner [17].

Meta-analysis and cohort studies have reported that breast cancer rates are higher among women diagnosed with type 2 diabetes mellitus (the most common form of this condition) than among their non-diabetic counterparts, particularly at post-menopausal stages [28–29]. Based on epidemiological studies, women with diabetes mellitus seem to be at greater risk of developing breast cancer during the pre-diabetes phase and because of low circulatory estrogen level [30–31]. It has been reported that the association between type 2 diabetes mellitus and breast cancer was significant among women with ER-positive tumors [32]. To improve the therapy and management of diabetic patients diagnosed with breast cancer, a better understanding of the interaction between AGEs in diabetes mellitus and ER-positive breast cancer cells is of great interest. Thus, in this present study, we investigated the biological impact of AGEs on the ER-positive MCF-7 breast cancer cells, on their cellular function, signal transduction, and RAGE and ER expression.

2. Materials and methods

2.1. Reagents

All reagents were obtained from Sigma-Aldrich (Dorset, UK), unless indicated otherwise.

2.2. Preparation of MG-BSA-AGEs

Methylglyoxal-derived bovine serum albumin advanced glycation endproducts (MG-BSA-AGEs) and non-modified BSA were prepared as described previously [17].

2.3. Culture of MCF-7 breast cancer cells

The MCF-7 breast cancer cell line was obtained from American Type Culture Collection (Manassas, VA, USA) and cultured in complete medium comprising Dulbecco's Modified Eagle's Medium (DMEM) supplemented with 10% heat-inactivated fetal bovine serum (FBS), 2 mM glutamine and antibiotics (100 μg/mL streptomycin and 100 IU/mL penicillin) at 37 °C in a saturated humid air/5% CO_2 incubator.

2.4. Cell proliferation assay

MCF-7 cells (2.5×10^4 mL) were seeded in 24-well plates (Nunc™, Fisher Scientific, Loughborough, UK) in complete medium. The experimental conditions were applied for 72 h of incubation as previously described [17]. Each condition was performed in duplicate, and each experiment was repeated independently three times. The untreated and MG-BSA-AGEs-treated cells were then counted using a Beckman-Coulter counter (Buckinghamshire, UK). The cell viability was evaluated using an automated cell counter TC10 (Bio-Rad, Munich, Germany), based on the trypan blue exclusion method.

2.5. Directional cell migration and invasion assays

The Boyden chamber system composed of Transwell® inserts (Nunc™) in a 24-well plate was used to assess MCF-7 cell migration and invasion across a porous membrane (8 μm pore size) coated with gelatin and a reconstituted basement membrane (Matrigel™; Becton Dickinson, Oxford, UK), respectively. Either gelatin (0.1% v/w) or growth-factor reduced Matrigel™ (1:6 dilution) was diluted in serum-free medium and then poured onto the porous membrane of the insert plate as described previously [17]. Each condition was performed in duplicate, and each experiment was repeated independently at least three times. The migrated or invaded cells were fixed with 4% paraformaldehyde, stained with a 0.1% solution of Giemsa, and counted using a Zeiss optical microscope.

2.6. Gelatin zymography

Matrix metalloproteinase (MMP) activities in the cell-culture media which had been used for cell invasion assay were evaluated. The medium was collected and centrifuged ($600 \times g$ for 15 min at 4 °C). Protein concentration was determined using the Bradford protein assay (Bio-Rad), and the samples (100 μg of protein) were mixed with an equal volume of non-reducing sample buffer. From protein concentration determination to the destaining of the gels, the zymography method used has been described previously [17]. In order to identify the corresponding MMP, in addition to their molecular size, recombinant human (rh) MMP-2 (ab81550) and rhMMP9 (ab82955) purchased from Abcam (Cambridge, UK) were analysed along with the protein samples. MMP gelatinase activity was detected as a white band on a dark background and quantified by densitometry using Image J software (http://rsbweb.nih.gov/ij/index.html).

2.7. Preparation of cell lysates and Western blot analysis

MCF-7 cells ($6 \times 10^5/2$ mL) were seeded in 6-well plates (Nunc™) in complete medium. After 48 h of incubation, the medium was renewed with serum-poor medium (SPM; medium supplemented with 2.5% FBS) for an additional 24-hour incubation, and MG-BSA-AGEs or non-modified BSA were added and incubated for different time periods (from 10 min to 72 h). Each condition was performed in duplicate, and each experiment was repeated independently three times. Cell lysate preparation, protein separation by 12% sodium dodecyl sulfate-polyacrylamide gel electrophoresis and transfer of separated proteins to polyvinylidene difluoride membranes were performed as previously described [17]. The membranes were then incubated overnight at 4 °C on a rotating shaker in the presence of primary antibody, which had been diluted in blocking buffer (1% BSA in Tris-buffered saline [TBS]–Tween]. Mouse monoclonal antibody against phospho-extracellular signal-regulated kinase (p-ERK1/2 [E-4], Tyr204 of ERK1, sc-7383; 1:1000 dilution), rabbit polyclonal antibodies to total ERK1/2 [C-16] (t-ERK1/2, sc-93; 1:1000), and mouse monoclonal antibodies to RAGE [E-1] (sc-74,473; 1:1000 dilution) were provided by Santa Cruz Biotechnology (Heidelberg, Germany). Mouse monoclonal antibodies to GAPDH [6C5] (ab8245; 1:2000 dilution), rabbit polyclonal antibodies

to estrogen receptor-β (ab5786; 1:1000) and rabbit monoclonal antibodies to estrogen receptor-α [E115] (ab32063; 1:1000) were purchased from Abcam (Cambridge, UK). Rabbit monoclonal antibodies to cleaved caspase-3 [5A1E] (#9664; 1000 dilution) and to caspase-3 [8G10] (#9665; 1000 dilution) were provided by Cell Signaling Technology (Danvers, MA, USA). The primary antibodies were detected with infrared fluorescent (red) IRDye® 680RD-conjugated goat anti-rabbit or (green) IRDye® 800RD-conjugated goat anti-mouse secondary antibodies (LI-COR Biosciences, Lincoln, NE, USA) diluted in TBS-Tween containing 3% BSA (1:1000 dilution) for 1 h at room temperature with continuous mixing. After five washes in TBS-Tween, the proteins were scanned and analyzed using the Odyssey CLx Scanner equipped with Image Studio software (LI-COR Biosciences).

2.8. Kinexus phospho-protein array analysis

MCF-7 cells (6×10^5/2 mL) were seeded in 6-well plates in complete medium. After 24-hour incubation, the medium was changed to SPM. After additional 24-hour incubation, 100 µg/mL MG-BSA-AGEs or non-modified BSA were added, and the cells were then incubated for 10 min at 37 °C. To determine the protein expression profiles of signaling components downstream of RAGE, a phospho-protein array analysis (Kinetworks PhosphoSite Screen, KPSS-1.3) was performed in triplicate by Kinexus Bioinformatics (Vancouver, Canada). Protein samples (500 µg) from the MG-BSA-AGE-treated or non-modified BSA-treated and untreated cells were extracted according to the manufacturer's instructions.

2.9. Flow cytometric analysis

MCF-7 cells (6×10^5/2 mL) were seeded in each well of a 6-well plate in complete medium. After 24-hour incubation, the medium was replaced with SPM for additional 24-hour incubation, and then 100 µg/mL MG-BSA-AGEs were added and incubated for 72 h. Each condition was performed in triplicate, and each experiment was repeated independently four times. The cells were washed with phosphate buffered saline (PBS) and then scraped to maintain the intact structure of RAGE (a transmembrane protein). The cells were washed with PBS and half of the cells had their membranes permeabilized with 0.1% Triton X-100 in PBS for 10 min following to fixation with 3.7% formaldehyde for 10 min. After centrifugation ($300 \times g$ for 10 min), 10^6 cells were re-suspended in 20 µL of PBS, and then 20 µg/mL mouse anti-RAGE (E-1) antibody or 2 µg of the mouse IgG$_1$ isotype control (ab91353 from Abcam) was added. The mixture was incubated on ice for 45 min, and then the excess antibody was removed by washing the cells twice with PBS, followed by centrifugation ($300 \times g$ for 10 min, at 4 °C). After the second centrifugation, the cells were re-suspended in 20 µL of PBS then 20 µg/mL of monoclonal anti-mouse antibody-FITC (Invitrogen, Paisley, UK) was added, and the mixture incubated on ice for 30 min. The RAGE expression level was measured using the FACS Diva analysis software from the FACS Canto Flow Cytometer (Becton Dickinson).

2.10. RNA extraction and quantitative real-time (qRT)-PCR

MCF-7 cells (6×10^5/2 mL) were seeded in 6-well plates in complete medium. After 24-hour incubation, the medium was replaced with SPM in the presence or absence of 100 µg/mL MG-BSA-AGEs or non-modified BSA and incubated for a further 72 h. Each condition was performed in duplicate, and each experiment was repeated independently three times. Total RNA was extracted using the RNeasy Mini Kit (Qiagen Inc., Valencia, CA, USA) to quantitatively monitor the expression of the human *MMP-9* (GenBank Accession No. NM_004994.2), *RAGE* (GenBank accession No. AB036432), *ER-α* (GenBank No. NM_001122740.1) and *ER-β* (GenBank accession No. NM_001437.2) mRNAs relative to the internal control 'house-keeping' gene *glyceraldehyde 3-phosphate dehydrogenase* (*GAPDH*, GenBank accession No. DQ403057)

mRNA using real-time PCR. Complementary DNAs (cDNAs) were produced from the total RNA extracts via reverse transcription using the Transcriptor first-strand cDNA synthesis kit (Roche Molecular Systems, Pleasanton, CA, USA), and the reaction was performed in a Tetrad2 Thermal Cycler (Bio-Rad). The sequences of the primer pairs (Invitrogen Life Technologies, Paisley, UK) were as follows: 5′-CGCTACCACCTCGAACTTTG-3′ (forward, F) and 5′-GCCATTCACGTCGTCCTTAT-3′ (reverse, R) for human *MMP-9*; F: 5′-GGC TGG TGT TCC CAA TAA GG-3′ and R: 5′-TCA CAG GTC AGG GTT ACG GTT C-3′ for human *RAGE*; F: 5′-TGG AGA TCT TCG ACA TGC TG-3′ and R: 5′-TCC AGA GAC TTC AGG GTG CT-3′ for human *ER-α*; F: 5′-CTC CAG CAG CAG GTC ATA CA-3′ and R: 5′-TCA GGC ATG CGA GTA ACA AG-3′ for human *ER-β*; and F: 5′-TGT CAT CAT ATT TGG CAG GTT-3′ and R: 5′-TTG GTA TCG TGG AAG GAC TCA-3′ for human *GAPDH*. The primers were designed using primer3 software (http://simgene.com/Primer3). The qRT-PCR was performed using a QuantiTect Reverse Transcription kit containing PCR SYBRGreen Master Mix (Applied Biosystems, Grand Island, NY, USA) and performed on a 7500 real-time PCR system (Applied Biosystems). For each analysis, a negative control was prepared using all reagents except the cDNA template. All reactions were performed in triplicate.

2.11. Confocal laser scanning microscopy

Cells (1×10^3) were grown in an 8-well µ-Slide (Ibidi, Planegg-Martinsried, Germany) in complete medium. After 24-hour incubation, the medium was replaced with SPM in the presence or absence of 100 µg/mL MG-BSA-AGEs or non-modified BSA and incubated for 6, 24, 48, and 72 h. Each condition was performed in triplicate. Cells were fixed with 3.7% formalin for 10 min at room temperature then washed twice with PBS and permeabilized with 0.1% Triton X-100 in PBS for 15 min after which cells were again washed twice with PBS. For ER-α detection, the cells were incubated overnight with rabbit anti-ERα polyclonal antibody. After washing with PBS, an additional mixture of cells and Alexa Fluor®-488-conjugated goat-anti-rabbit antibody (Thermo Fisher Scientific, USA) was produced to visualize ER-α. Nuclei were stained with 0.5 µg/mL Hoechst 33342 dye. ER-α expression and location was examined by confocal scanning microscopy using a Zeiss LSM 780 system (Carl Zeiss, Jena, Germany) equipped with 40× oil-immersion objective.

2.12. ER-α transcription factor activation assay

MCF-7 cells (6×10^5/2 mL) were seeded in 6-well plates in complete medium. After a 24-hour incubation, the medium was replaced with SPM in the presence or absence of 100 µg/mL MG-BSA-AGEs or non-modified BSA and further incubated for 48 h. Each condition was performed in duplicate, and each experiment was repeated independently three times. Nuclear proteins were extracted using nuclear protein extraction kit according to the manufacturer's instructions (#ab113474, Abcam). Nuclear proteins containing ER-α were assessed for ER-α transcription factor activation assay according to the manufacturer's instructions (#ab207203, Abcam) based on ER-α bound to a specific double stranded DNA sequence containing the ER consensus binding site (5′-GGTCACAGTGACC-3′).

2.13. RAGE neutralization

Cells were treated with an anti-RAGE antibody to neutralize the RAGE receptors according to the experimental conditions previously described in [17]. Briefly, MCF-7 cells were seeded in 6-well plates in complete medium (as described above for the Western blots). The medium was replaced with SPM, and then 20 µg/mL mouse monoclonal anti-RAGE [E-1] antibody or 20 µg/mL of IgG$_1$, which was used as an isotype control, were added. After 2-h incubation, the cells were treated with 100 µg/mL MG-BSA-AGEs for 10 min or 72 h at 37 °C, and then
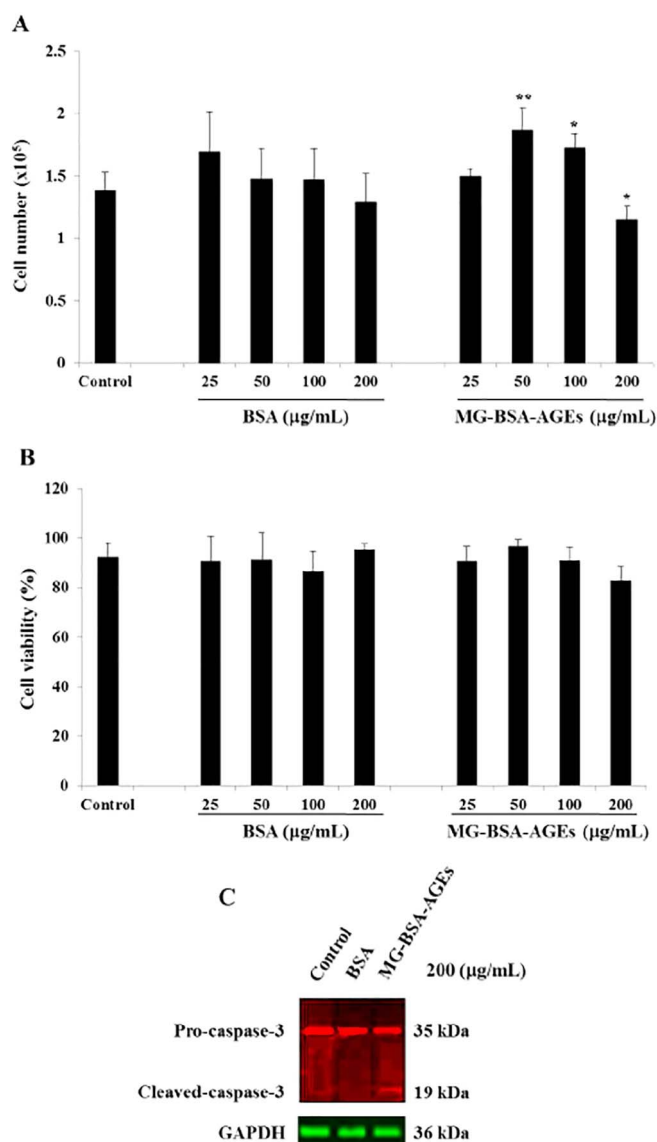
Fig. 1. Effects of MG-BSA-AGEs and non-modified BSA on (A) the proliferation and (B) the viability of MCF-7 breast cancer cells. The cells were treated with 25–200 µg/mL MG-BSA-AGEs or non-modified BSA for 72 h. Cell number (A) and cell viability (B) were determined using an automated cell counter and the trypan blue exclusion method, respectively. Control comprises untreated cells. The results are presented as mean ± SD ($n = 3$). (*) and (**) signify a statistically significant difference ($p < 0.05$ and $p < 0.01$ respectively) compared with the control. (C) Representative Western blot analysis showing the cleavage of pro-caspase-3 induced by 200 µg/mL MG-BSA-AGEs while no cleaved-caspase-3 was detected in untreated cells or cells treated with 200 µg/mL non-modified BSA after 72-hour incubation. GAPDH was used as the loading control.

the proteins were extracted for Western blotting. Each condition was performed in triplicate, and each experiment was repeated independently three times.

2.14. Statistical analysis

The results are expressed as the mean ± standard deviation (SD). Data points were collected for a minimum of three independent experiments. An unpaired Student's t-test was used to compare two groups and a value of $p < 0.05$ considered significant.

3. Results

3.1. MG-BSA-AGEs modulate MCF-7 cell proliferation

We first evaluated the biological impact of increasing concentrations (25–200 µg/mL) of either non-modified bovine serum albumin (BSA) or MG-BSA-AGEs on ER-positive breast cancer cell line MCF-7 proliferation, key cellular event involved in breast cancer development (Fig. 1). Compared to the untreated control cells, MG-BSA-AGEs increased then decreased MCF-7 cell proliferation (producing a bell-shaped curve) with peak stimulation in the presence of 50 and 100 µg/mL MG-BSA-AGEs (35% increase, $p < 0.01$) (Fig. 1A). At the lowest concentration (25 µg/mL), MG-BSA-AGEs had no effect on cell proliferation, whereas a marked inhibition of cell growth (17.0% decrease, $p < 0.05$) was observed at the highest concentration (i.e. 200 µg/mL) of MG-BSA-AGEs compared to the untreated control cells (Fig. 1A). Furthermore, the percentage of cell viability was determined by the trypan blue exclusion method (Fig. 1B). Under all conditions tested, a high percentage of cell viability was observed, and neither MG-BSA-AGEs nor non-modified BSA exerted cytotoxic effects (Fig. 1B).

We sought to determine the molecular mechanism underlying the inhibitory effects mediated by 200 µg/mL MG-BSA-AGEs on cell proliferation. After 72 h of incubation, whole proteins were extracted from untreated MCF-7 cells and cells treated with either 200 µg/mL non-modified BSA or MG-BSA-AGEs for Western blot analysis. Targeting pro-caspase-3 activation, responsible of the hallmarks of the programmed cell death (i.e. apoptosis), we detected cleaved caspase-3 (200 µg/mL) in MG-BSA-AGEs-treated cells while no cleaved caspase-3 was detected in untreated cells and cells treated with 200 µg/mL non-modified BSA (Fig. 1C).

3.2. MG-BSA-AGEs increase MCF-7 cell migration without affecting cell invasion

Having established that MG-BSA-AGEs enhance MCF-7 cell proliferation, their effect on MCF-7 cell migration, a key cellular function involved in cancer progression, was assessed. The Boyden chamber assay was used to evaluate the effect of the MG-BSA-AGEs on MCF-7 cell migration, based on a directional approach. MCF-7 cells were incubated in the presence of non-modified BSA or MG-BSA-AGEs at increasing concentrations (25–200 µg/mL) for 24 h (Fig. 2). Representative photomicrographs of the stained MCF-7 cells that migrated through the porous membrane at the end of the 24-hour treatment without (Fig. 2A) or with either 100 µg/mL non-modified BSA (Fig. 2B) or 100 µg/mL MG-BSA-AGEs (Fig. 2C) are shown in Fig. 2. At all concentrations tested, non-modified BSA had no effect on MCF-7 directional cell migration compared to the control (Fig. 2D). With an increasing concentration, MG-BSA-AGEs increased then decreased directional MCF-7 cell migration (producing a bell-shaped curve) with peak stimulation in the presence of 100 µg/mL MG-BSA-AGEs (2.1-fold; $p < 0.001$) compared to the control (Fig. 2D). At the lowest (25 µg/mL) and the highest (200 µg/mL) concentrations, the MG-BSA-AGEs did not significantly change the number of migrated cells compared to untreated control cells (Fig. 2D).

Although MCF-7 cells are known for their low invasive and metastatic potential [33], the invasion method consisted of the Boyden chamber assay with the porous membrane coated with growth factor-reduced Matrigel™ was used to determine whether the addition of MG-BSA-AGEs would stimulate cell invasiveness. After 24 h of incubation, MCF-7 cells were not able to invade the porous membrane at all concentrations of MG-BSA-AGEs used (25–200 µg/mL; data not shown). The lack of invasive potential was confirmed by the absence of active forms of matrix metalloproteinases (MMP)-9 and MMP-2, key enzymes involved in the invasive process through degradation of extracellular matrix proteins, revealed using gelatin-substrate zymography from MCF-7 cell-condition medium (Fig. 2E). However, compared with the
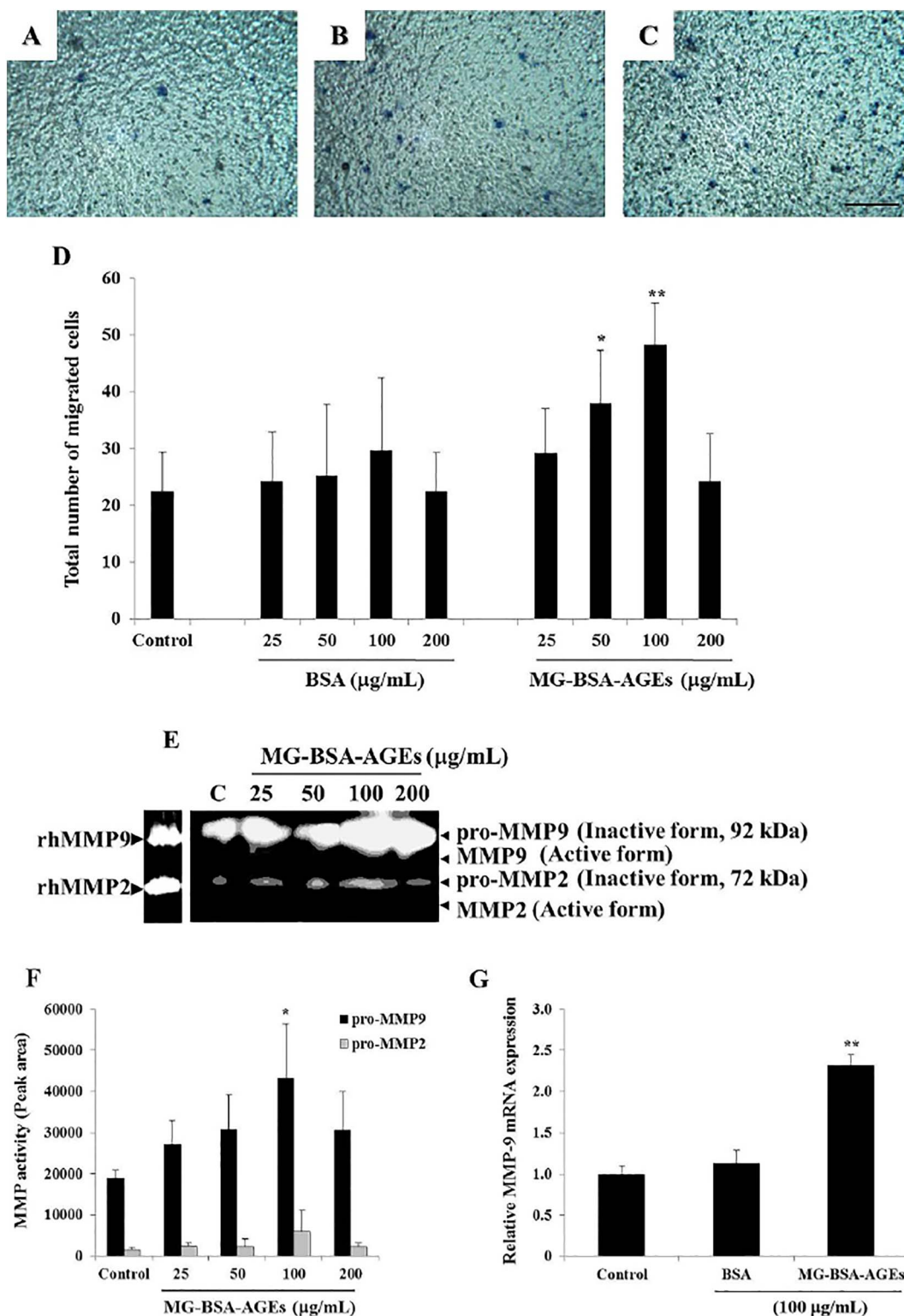
Fig. 2. Effects of MG-BSA-AGEs and non-modified BSA on the directional migration of MCF-7 breast cancer cells and on gelatinase (MMP-9/MMP-2) activity. Representative photomicrographs (×100 magnification) showing MCF-7 cells that migrated across a 0.1% gelatin-coated porous membrane after 24 h of incubation in the absence (A) or the presence (B) of 100 μg/mL non-modified BSA or (C) 100 μg/mL MG-BSA-AGEs. Scale bar = 100 μm. (D) Quantification of the number of migrated untreated cells and cells treated with 25–200 μg/mL of non-modified BSA or MG-BSA-AGEs. The results are presented as the mean ± SD ($n = 4$). (E) Representative gelatine zymographic analysis showing the MMP-9 and MMP-2 activities from 25 to 200 μg/mL of MG-BSA-AGE-treated MCF-7 cell-condition media, compared with untreated cell-condition medium (control). The gels revealed gelatinolytic activities of the inactive form of MMP-9 (pro-MMP-9) and MMP-2 (pro-MMP-2), identified by their respective recombinant human rhMMP. (F) Quantification of relative gelatinolytic activity of pro-MMP-9 and of pro-MMP-2 expressed as relative activity, which was calculated as a ratio of the control. The results are presented as the mean ± SD ($n = 3$). (G) Relative expression of MMP-9 mRNA was determined using qRT-PCR analysis in MCF-7 cells following a 24 hour-treatment with either 100 μg/mL non-modified BSA or MG-BSA-AGEs, calculated as a ratio of GAPDH mRNA and normalized to the control. The results are presented as the mean ± SD ($n = 3$). (*) and (**) signify a statistically significant difference ($p < 0.05$ and $p < 0.01$ respectively), compared with the control.
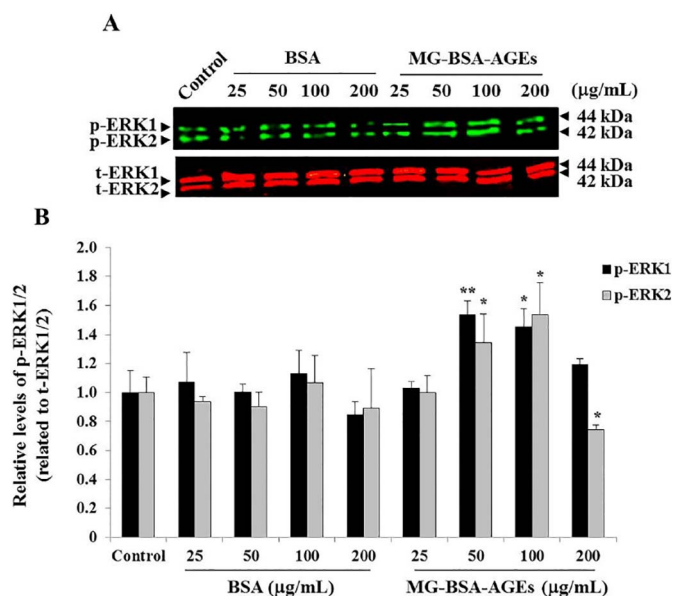
Fig. 3. Effect of MG-BSA-AGEs on the phosphorylation of ERK1/2 in MCF-7 cells. (A) Representative Western blot analysis showing the phosphorylation of ERK1/2 (p-ERK1/2) induced by increasing concentrations (25–200 μg/mL) of either non-modified BSA or MG-BSA-AGEs after a 10-minute incubation compared to the untreated control cells. (B) The bar graph shows the expression of p-ERK1/2 relative to control cells given an arbitrary value of 1.0 using total ERK1/2 (t-ERK1/2) as the loading control. The results are presented as mean ± SD ($n = 3$) where (*) and (**) signify a statistically significant difference ($p < 0.05$ and $p < 0.01$ respectively), compared with the control.

pro-MMP-9 activity in untreated MCF-7 cell-condition medium (control), treatment with 100 μg/mL MG-BSA-AGEs significantly enhanced pro-MMP-9 activity (2.26-fold, $p < 0.05$), which is the precursor and inactive form of MMP-9 (Fig. 2F). This pro-MMP-9 capacity in lysing gelatin substrate is believed to be due to the exposure of its intrinsic activity by autocatalytic cleavage [34]. In addition, performing qRT-PCR after 24-hour incubation, 100 μg/mL MG-BSA-AGEs significantly up-regulated MMP-9 mRNA (2.2-fold, $p < 0.01$) as compared to untreated control cells (Fig. 2G). No change of MMP-9 mRNA was observed in non-modified BSA-treated cells (Fig. 2G).

3.3. MG-BSA-AGEs increase the phosphorylation of signaling proteins

To assess the effect of either non-modified BSA or MG-BSA-AGEs (25-200 μg/mL) on signaling pathways in cultured MCF-7 cells, Western blotting was performed to determine the levels of ERK1/2 phosphorylation (p-ERK1/2) after a 10-minute treatment, optimal incubation time defined from pilot studies (data not shown). Non-modified BSA had no effect on the ERK1/2 phosphorylation in MCF-7 cells at any of the concentrations used, compared to untreated control cells (Fig. 3). In contrast, MG-BSA-AGEs modulated the level of ERK1/2 phosphorylation in a dose-dependent manner (Fig. 3A). The addition of 50 μg/mL or 100 μg/mL MG-BSA-AGEs induced maximal expression of p-ERK1/2 (1.4-fold) compared to the control (Fig. 3B). At the highest concentration (200 μg/mL), MG-BSA-AGEs significantly decreased ERK2 phosphorylation (0.75-fold, $p < 0.05$, Fig. 3B).

A wider investigation of the proteins phosphorylated in response to MG-BSA-AGEs/RAGE interaction was also performed using KPSS-1.3 phospho-protein array analysis. A total of 35 phospho-proteins were analyzed in whole cell lysates of untreated MCF-7 cells (control, Fig. 4A) or cells treated with 100 μg/mL MG-BSA-AGEs (Fig. 4B) or 100 μg/mL non-modified BSA (Fig. 4C). Compared to Western blot analysis, the quantitative immunoblots showed that the MG-BSA-AGEs induced 1.17-fold and 1.3-fold increases in p-ERK1 and p-ERK2 expression, respectively, compared to untreated control cell lysates (Fig. 4D). The MG-BSA-AGEs increased phosphorylation of mitogen-

activated protein kinase (MAPK)/ERK protein-serine kinase 1/2 (MKK1/2), an upstream kinase activator of ERK1/2, and of cAMP response element binding protein 1 (CREB1), which were reported to be associated with breast cancer development [27], by 2.04-fold and 1.98-fold compared to untreated control cells, respectively (Fig. 4D).

The analysis of the KPSS-1.3 phospho-protein array also included assessment of the phosphorylation of protein-serine kinase C (PKC) isoforms, such as PKCα, PKCα/β2, PKCε, and PKCδ, which have been shown to play different roles in breast cancer progression [35]. The 10-minute treatment with MG-BSA-AGEs induced a down-regulation of the phosphorylation of PKCε (Fig. 4B and E), whereas non-modified BSA up-regulated PKCε phosphorylation by 1.75-fold compared to untreated control cells (Fig. 4B and E). Compared to the control (Fig. 4A), the cells treated with MG-BSA-AGEs also showed a 50% decrease in the phosphorylation of PKCα, PKCα/β2, and PKCδ (Fig. 4B and E). The phosphorylation of mitogen- and stress-activated protein-serine kinase 1 (Msk1), an activated downstream kinase of ERK1/2 and p38 pathways involved in cell survival, proliferation and differentiation, and adducin α, a cytoskeleton protein that dissociates from F-actin and spectrin during cell migration, was also down-regulated by 50% (Fig. 4E) in MCF-7 cells after treatment with MG-BSA-AGEs (Fig. 4B) compared to untreated control cells (Fig. 4A). However, the level of phosphorylation of PKCα, PKCα/β2, PKCδ, Msk1 and adducin α detected in MG-BSA-AGEs-treated MCF-7 cells was 20-50% lower than the levels of these phospho-proteins detected in non-modified BSA-treated MCF-7 cells (Fig. 4E).

3.4. MG-BSA-AGEs up-regulate RAGE and ER expression in MCF-7 cells through RAGE

To check whether MG-BSA-AGEs (100 μg/mL) up-regulate expression of RAGE and estrogen receptors, two types of receptors described to play major roles in breast cancer development and progression [36–37]; Western blotting, qRT-PCR, and FACS analysis were applied. MG-BSA-AGEs up-regulated RAGE and estrogen receptor (ER)-α/β protein expression in a time-dependent manner (Fig. 5A). At all incubation times (24, 48 and 72 h), in untreated control conditions or in the presence of non-modified BSA (100 μg/mL), no change of RAGE protein expression was observed as compared to RAGE basal expression level detected in untreated control cells at 24 h. Compared to the RAGE basal expression level, MG-BSA-AGEs up-regulated by 1.3-fold and 1.5-fold RAGE expression at 48 and 72-hour post-treatment, respectively (Fig. 5B). With regards to ER-α, its expression increased by 1.3-fold with (at all incubation times) or without addition of non-modified BSA (48–72 h of treatment), compared to basal ER-α expression level detected in untreated control cells at 24 h. At all incubation times, MG-BSA-AGEs enhanced ER-α protein expression in a time-dependent manner (Fig. 5A). MG-BSA-AGEs increased ER-α protein expression by 1.3-, −1.5 and −1.7-fold after 24, 48 and 72 h, respectively; with a significant difference ($p < 0.05$) between 48 and 72 hour time-points, as compared to the basal ER-α expression in untreated control cells at 24 h (Fig. 5B). With regards to ER-β, its expression increased (1.6-fold, $p < 0.01$) in untreated conditions after 48 and 72 h, compared to basal ER-β expression detected in untreated control cells after 24 h. Over the time, the addition of non-modified BSA increased ER-β expression by 1.6-fold after 24 h then decreased progressively reaching the basal ER-β expression after 72 h as compared to the ER-β basal expression level detected in untreated control cells at 24 h (Fig. 5B). Conversely, a significant decrease in ER-β expression (0.75-fold and 0.87-fold) was observed after cells were treated with MG-BSA-AGEs for 24 and 48 h respectively. However, an increase in ER-β expression (1.26-fold) was only observed after 72 h compared with the respective basal expression detected in untreated control cells at 24 h (Fig. 5B). The mRNA expression of RAGE, ER-α and ER-β were monitored using qRT-PCR after 72 h of treatment. Compared with the basal level obtained in untreated cells, no statistically significant differences were observed in the non-
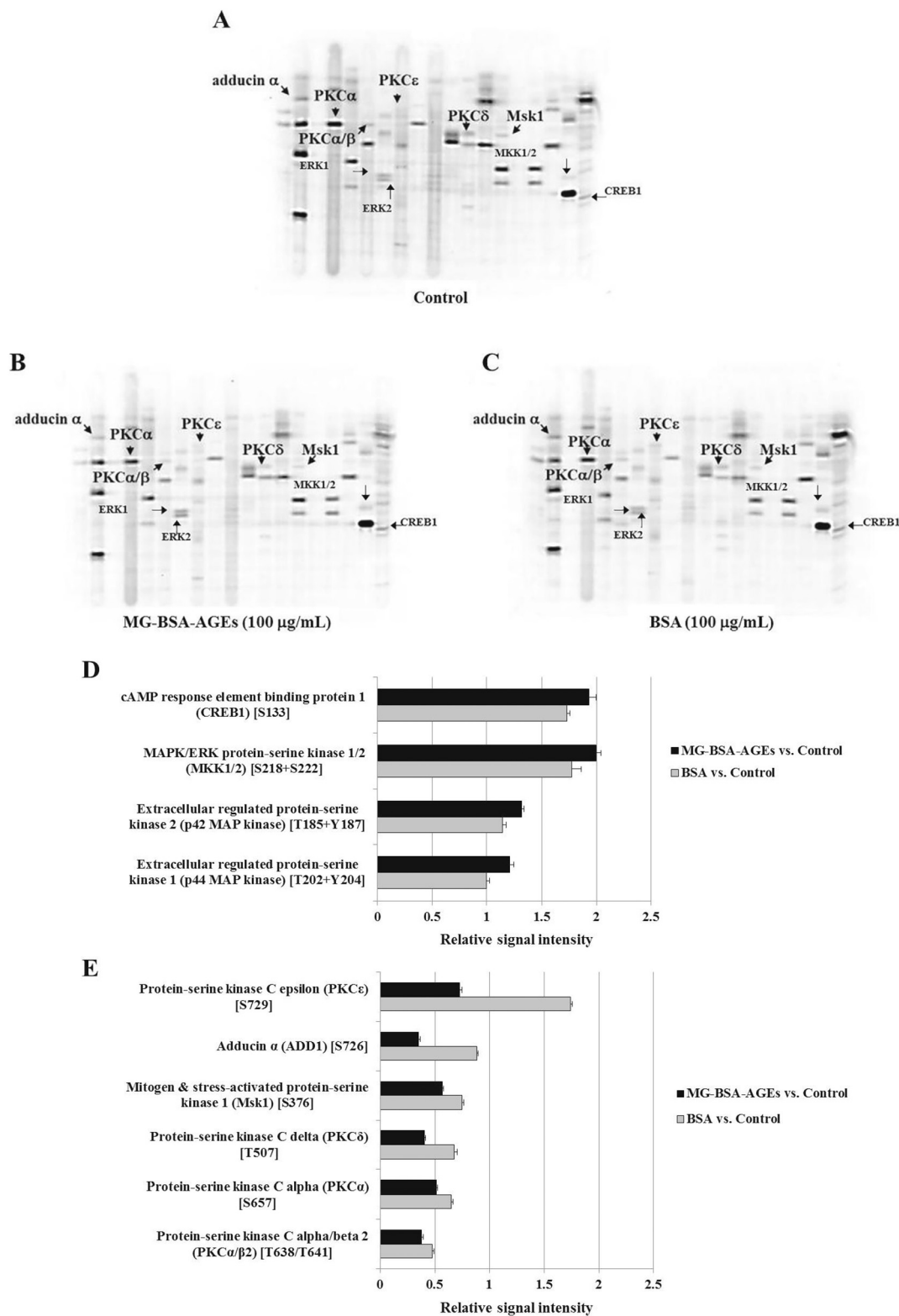
Fig. 4. Effects of MG-BSA-AGEs on the phosphorylation of signaling proteins, including MAPK, CREB1 and PKC, in MCF-7 cells. Multi-immunoblotting of 35 phospho-proteins expressed in untreated MCF-7 cells (A), cells treated with 100 μg/mL MG-BSA-AGEs (B) or cells treated with 100 μg/mL non-modified BSA (C), for 10 min. (D) The bar graph shows the relative levels of phospho-cAMP responsive element binding protein-1 (CREB1) and phospho-MAPK expressed in counts per minutes, which was calculated as a ratio of relative signal intensity to the levels detected in the untreated control cells. (E) The bar graph shows the relative expression of phospho-adducin α, phospho-Msk1 and phospho-PKC isoforms.

modified BSA-treated cells (Fig. 5C). However, in the MG-BSA-AGEs-treated cells, significant increases in the levels of RAGE (1.3-fold, $p < 0.001$), ER-α (3.3-fold, $p < 0.01$) and ER-β (2.1-fold, $p < 0.001$) transcripts were obtained (Fig. 5C), supporting the up-regulation of the

respective protein expression observed using Western blotting (Figs. 5B).

FACS analysis was performed to detect RAGE expression on the surface or inside (after membrane permeabilization) the MCF-7 cells
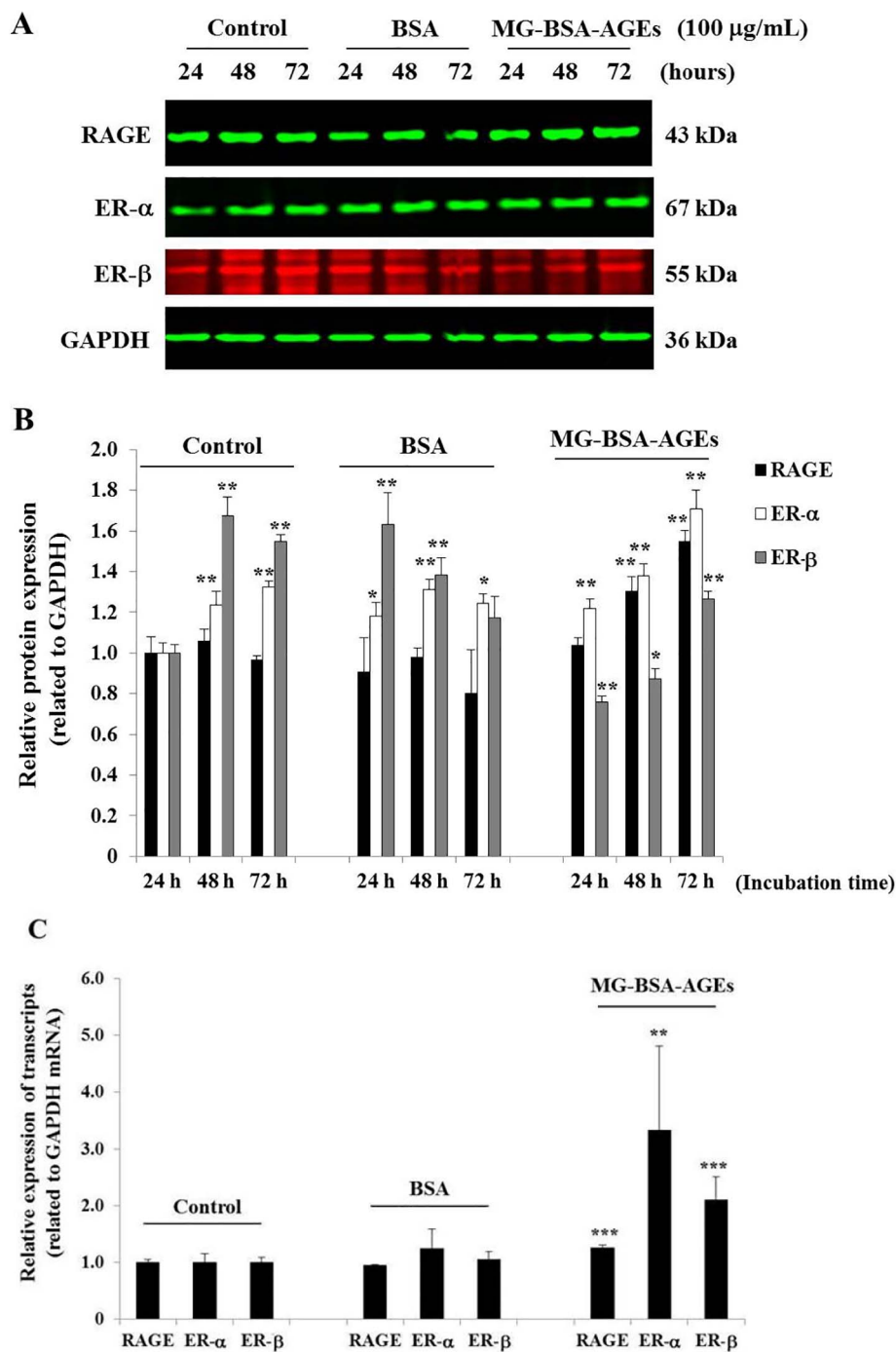
A

B

C

Fig. 5. Time-course of RAGE, ER-α and ER-β protein and mRNA expression in MCF-7 breast cancer cells treated with MG-BSA-AGEs. (A) Representative Western blot showing the effect of 100 µg/mL non-modified BSA or 100 µg/mL MG-BSA-AGEs on RAGE, ER-α and ER-β protein expression in MCF-7 cells after incubation for 24, 48 or 72 h compared to the untreated control cells. (B) The bar graph shows the relative protein expression of RAGE, ER-α and ER-β calculated as a ratio of GAPDH expression (the loading control) and normalized to the control. (C) Relative expression of the RAGE, ER-α and ER-β mRNAs was determined using qRT-PCR analysis in MCF-7 cells following a 72-hour treatment with 100 µg/mL non-modified BSA or 100 µg/mL MG-BSA-AGEs, calculated as a ratio of GAPDH mRNA and normalized to the control. The results are presented as the mean ± SD ($n = 3$) where (*), (**) and (***) signify a statistically significant difference ($p < 0.05$, $p < 0.01$ and $p < 0.001$ respectively) compared to the control.

after 72 h of incubation with 100 µg/mL MG-BSA-AGEs or non-modified BSA. Compared with the isotype (negative) control, RAGE was detected on the surface of untreated MCF-7 cells, and the addition of MG-BSA-AGEs to MCF-7 cells decreased RAGE expression on the cell surface (Fig. 6A). A greater amount of intracellular RAGE was observed in untreated cells, but concomitant increase in intracellular RAGE expression occurred in the MG-BSA-AGE-treated cells (Fig. 6B).

Considered as the main ER influencing MCF-7 cell response to estrogens, only ER-α location was visualized using confocal fluorescence microscopy. Weak expression of ER-α was noticed in the cytoplasm and the nucleus compared to the control untreated cells (Fig. 6C, top row). Compared to ER-α basal expression detected in untreated cells after 6 h of incubation, MCF-7 cells treated with 100 µg/mL non-modified BSA led to a concomitant increase of ER-α expression in both cytoplasmic

and nuclear compartments observed after 48 h of treatment (Fig. 6C, middle row). This supports the significant increase in ER-α expression noticed using Western blotting (Fig. 5B). In contrast to untreated MCF-7 cells and cells treated with non-modified BSA, 100 µg/mL MG-BSA-AGEs enhanced ER-α expression following 6 h of treatment in both cytoplasmic and nuclear compartments (Fig. 6C, bottom row). Cytoplasmic ER-α was predominantly high after 24 and 72 h of treatment with MG-BSA-AGEs, while nuclear ER-α were mainly found sequestrated into small nucleoli. After 48 h of treatment with MG-BSA-AGEs, nuclear ER-α expression was predominantly high and mainly sequestrated into one nucleolus site for most of the cells, considered as a site of high transcriptional activity (Fig. 6C, bottom row). At similar conditions (48 hour-treatment with MG-BSA-AGEs vs. non-modified BSA), ER-α transcription factor activation based on the recognition of the
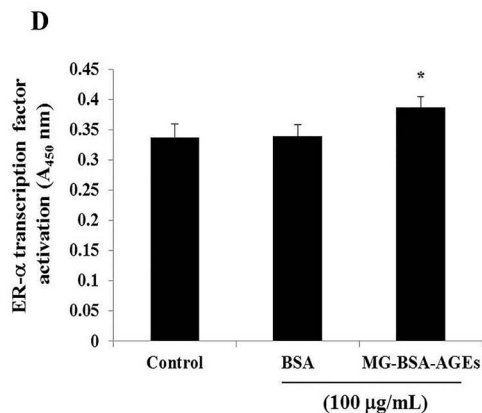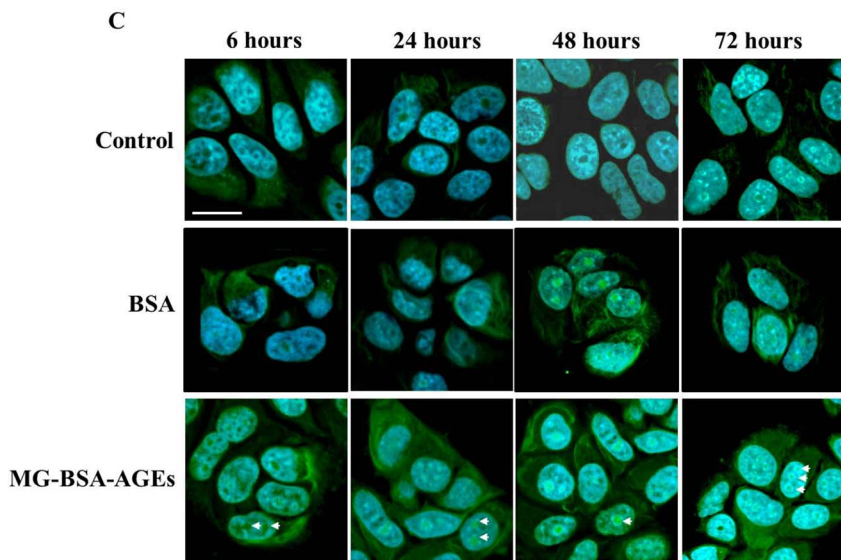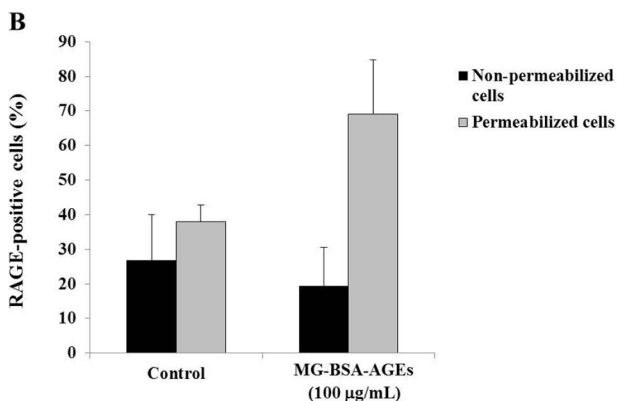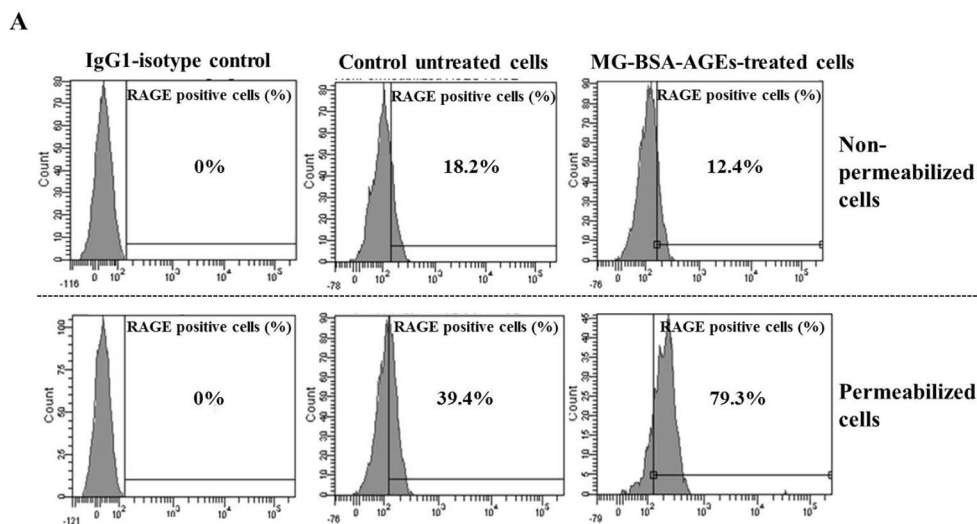
Fig. 6. Effect of MG-BSA-AGEs on cellular distribution of RAGE and ER-α expression in MCF-7 cells. (A) Representative FACS results showing the effect of 100 μg/mL MG-BSA-AGEs on FITC-conjugated RAGE expression on the surface of non-permeabilized MCF-7 cells or inside the permeabilized MCF-7 cells after 72 h of incubation compared to the untreated control. An isotype control antibody FITC-conjugated IgG_1 was used to establish the FACS instrument settings. (B) The bar graph shows mean ± SD of the percentage of RAGE-positive cells in MG-BSA-AGEs-treated permeabilized and non-permeabilized MCF-7 cells, compared to untreated control cells ($n = 4$). (C) Representative photomicrographs showing cytoplasmic and nuclear locations of ER-α protein expression (green fluorescence) in untreated MCF-7 cells (top row), in MCF-7 cells treated with either 100 μg/mL non-modified BSA (middle row) or MG-BSA-AGEs (bottom row) after different incubation times (from 6 to 72 h). White arrows indicate ER-α sequestration into the nucleoli. Scale bar = 20 μm. (D) The bar graph shows mean ± SD for the absorbance (measured at 450 nm) reading of the level of ER-α transcription factor activation in MG-BSA-AGEs-treated MCF-7 cells after 48 h of treatment, compared to non-modified BSA-treated cells and untreated control cells ($n = 3$). (*) signifies a statistically significant difference ($p < 0.05$) compared with the control.
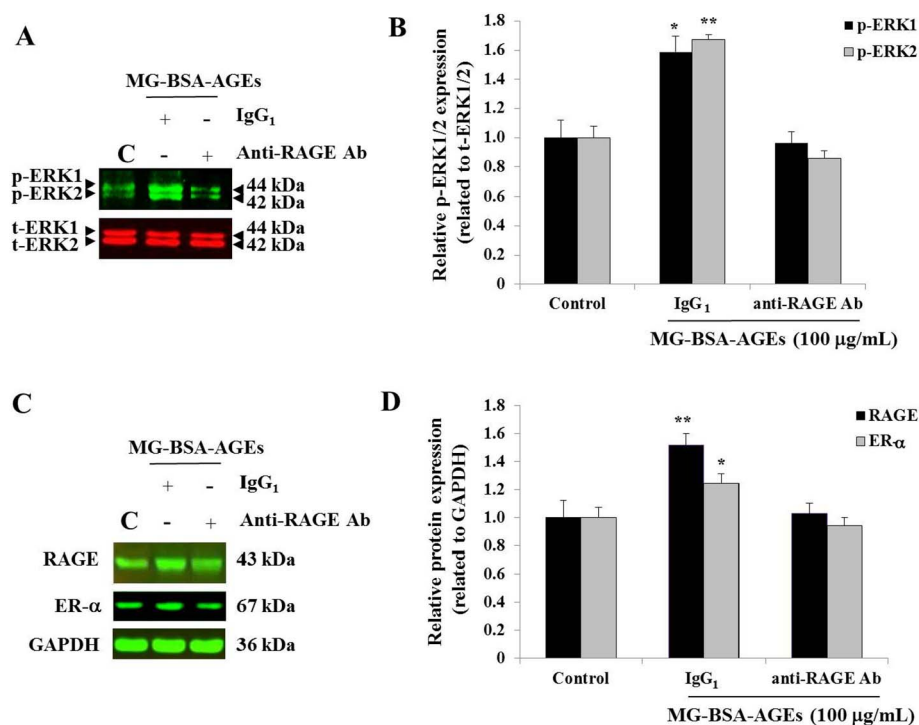
Fig. 7. RAGE mediates MG-BSA-AGE-induced p-ERK1/2, RAGE and ER-α expression in MCF-7 cells. Representative Western blot analysis showing the loss of MG-BSA-AGE-induced phosphorylation of (A) ERK1/2 and (C) RAGE and ER-α after the blockade of RAGE by an anti-RAGE antibody compared to isotype control IgG$_1$-treated cells. Bar graphs show the relative expression of (B) ERK1/2 and (D) RAGE and ER-α calculated as ratio to the total ERK1/2 and GAPDH, the respective controls. The results are presented as mean ± SD ($n = 3$). (*) and (**) signify a statistically significant difference ($p < 0.05$ and $p < 0.01$ respectively) compared with the control.

antibody directed to ER-α bound to a specific double stranded DNA sequence containing the ER consensus binding site was assessed. Compared to ER-α, transcription factor activation seen in untreated MCF-7 cells or cells treated with non-modified BSA, the level of ER-α transcription factor activation increased (1.15-fold, $p < 0.05$) in MCF-7 cells treated with MG-BSA-AGEs for 48 h of incubation (Fig. 6D).

To check whether MG-BSA-AGEs stimulated MCF-7 cells through their major receptor RAGE, the cells were pre-treated with either a neutralizing RAGE antibody to block all the RAGE molecules or with an isotype control IgG1 used as a negative control (Fig. 7). After the blockade of RAGE function using anti-RAGE antibody, MG-BSA-AGEs lost its stimulatory effects on ERK1/2 phosphorylation and on RAGE and ER-α expression, whereas MG-BSA-AGEs increased ERK1/2 phosphorylation and up-regulated RAGE and ER-α expression in IgG$_1$-treated cells, demonstrating that MG-BSA-AGEs act through RAGE (Fig. 7).

4. Discussion

Diabetes mellitus and cancer are causes for concern due to their high incidence in Western countries and, more recently, in developing countries. Currently, there is growing evidence of molecular links between diabetes mellitus and breast cancer [15–17]. Mainly generated under hyperglycemic conditions and by active cancerous cells, AGEs represent the main toxic and inflammatory metabolites playing a pivotal role in the cause-and-effect between diabetes and cancer. Although ER-positive breast cancer has a better prognosis, a study reported a direct correlation between type 2 diabetes and ER-positive breast cancer onset and development [32,38]. In order to improve our understanding of the role of AGEs on ER-positive breast cancer progression, this study investigated the biological effects of MG-BSA-AGEs on ER-positive MCF-7 human breast cancer cell line. Here, we show that 50-100 μg/mL MG-BSA-AGEs slightly increase MCF-7 cell proliferation and migration without affecting cell invasion, while 200 μg/mL MG-BSA-AGEs induced apoptosis leading to the cleavage of caspase-3. Furthermore, the MG-BSA-AGEs increase expression of RAGE, ER-α and ER-β, and the phosphorylation of key signaling proteins including ERK1/2. In addition, the blockade of RAGE using a neutralizing RAGE

antibody reverses MG-BSA-AGEs-induced ERK1/2 phosphorylation and MG-BSA-AGEs-induced RAGE and ER-α up-regulation. Altogether, this study demonstrates that the pro-tumorigenic effects of AGEs on ER-positive breast cancer cell line MCF-7 characterized by ERK1/2 phosphorylation, RAGE and ER-α up-regulation are mediated through RAGE, which likely suggests an increase of sensitivity of ER-positive breast cancer cells to AGEs and estrogens for breast cancer development.

In this study, MCF-7 cells were treated with various concentrations of MG-BSA-AGEs or non-modified BSA and their effects on breast cancer cellular functions such as proliferation, migration, invasion and signaling pathways were determined. At concentrations of 50 and 100 μg/mL, the MG-BSA-AGEs significantly increased cell growth and motility, but had an inhibitory mitogenic effect observed at 200 μg/mL. These dose-response effects showed a bell-shaped curve, suggesting that activation of a receptor whose optimal oligomerization occurs in the presence of 50-100 μg/mL of MG-BSA-AGEs. These findings were similar to our previous study reporting the bell-shaped dose-response of MG-BSA-AGEs on MDA-MB-231 breast cancer cells in a RAGE-dependent manner [17]. However, at higher concentration of MG-BSA-AGEs (200 μg/mL), an impediment of RAGE oligomerization may occur as demonstrated by other studies using biophysics and biochemical technologies, which can explain the decrease of the MCF-7 cell proliferation [39–40]. In addition, similar high concentration of AGEs (200 μg/mL) have been demonstrated to induce apoptosis in pancreatic islet endothelial cells leading to the cleavage of caspase-3 and of poly(ADP-ribose) polymerase (PARP) proteins, both hallmarks of apoptosis [41].

Using the gelatin zymography method, the activities of the enzymes involved in basement membrane degradation allowing the cells to invade, such as the gelatinases MMP-2 and MMP-9 were assessed. Both MMP-2 and MMP-9 activities were evaluated in the conditioned medium from the MCF-7 cells after the invasion assay in the presence or absence of different concentrations of non-modified BSA or MG-BSA-AGEs. Under all conditions tested, non-modified BSA and MG-BSA-AGEs did not activate MMP-2 and MMP-9. However, MG-BSA-AGEs significantly enhanced the amount of enzymatically inactive state pro-MMP-9 and up-regulated MMP-9 gene expression revealed using qRT-PCR. This absence of gelatinase MMP activation reinforces the MCF-7 weak invasive capacity only, while MG-BSA-AGEs-induced cell

migration can occur without MMP activation as demonstrated by Dufour et al. [42] reporting that COS cell (fibroblast-like cell line) migration was enhanced in a non-proteolytic manner by latent pro-MMP-9.

We also showed that 100 μg/mL MG-BSA-AGEs up-regulated RAGE expression in MCF-7 cells, particularly after 48 and 72 h of treatment. It is noteworthy that RAGE up-regulation occurred in the intracellular forms of the receptor while a slight decrease of RAGE expression was observed on the cell surface. This observation underlines the internalization of RAGE over time as previously reported using Chinese hamster ovary cells (CHO-K1) and neuro-2 cells [43]. This RAGE internalization was demonstrated to be required to mediate intracellular response [43]. Furthermore, in this study, RAGE up-regulation induced by MG-BSA-AGEs was confirmed by the increase of mRNA RAGE transcripts monitored after 72 h of treatment. These findings are supported by other studies [44], where overexpression of the RAGE mRNA and protein in human vascular endothelial cells were observed following treatment with MG-BSA-AGEs. The same study also demonstrated a stimulatory effect on RAGE gene expression at the transcript level by identifying an AGE-responsive element in a region upstream from the transcription start site of the human RAGE gene [44]. Thus, the decreased expression of RAGE on the cell surface explains the modest biological effect of AGEs on breast cancer cells.

This present investigation of effects of AGEs on ER-positive breast cancer cells led us to monitor nuclear receptor ER-α and ER-β expression, two transcription factors that mediate estrogen signaling, in MG-BSA-AGEs-treated MCF-7 cells at different time-points. MG-BSA-AGEs increased ER-α expression in MCF-7 cells with the incubation time, while MG-BSA-AGEs down-regulated ER-β expression at 24–48 h after treatment followed by up-regulation of ER-β expression at 72-hour post-treatment. This up-regulation of RAGE, ER-α and ER-β induced by MG-BSA-AGEs detected at 72-hour post-treatment was confirmed by the up-regulation of their respective transcripts mRNA. In response to estrogen, activation of ER-α signaling results in stimulation of breast cancer cell growth, differentiation and breast cancer progression, while ER-β has been reported to exert a negative regulatory role for ER-α and an anti-proliferative role in breast cancer [45–46]. These differential effects of AGEs on ER-α and ER-β expression, encoded by independent genes, suggest that activation of different regulatory mechanisms including epigenetic changes are influenced under transient high glucose or through hypermethylation of the *ESR2* promoter associated with a marked decrease of ER-β [47–48]. This might explain the altered gene expression of ER mediated by AGEs. In addition, the different level of ER-β expression between the protein and transcript detected in untreated cells can be explained by a transcriptional regulation between ER-β mRNA transcript and the protein expressed. A study reported that ER-β expression is often down-regulated in cancer compared to normal cells and is negatively regulated by the microRNA miR-92 in MCF-7 cells [49]. To understand better this transcriptional regulation, a study on miR-92 might help clarify this negative regulation on ER-β protein expression observed in certain experimental conditions. Furthermore, using human microvascular endothelial cells, a previous study showed that ER-α activation triggered the activation of the SP1 transcription factor, known to regulate the expression of pro-oxidative and pro-inflammatory genes including the stimulation of RAGE gene expression [50]. This latter study also demonstrated a differential effect of ER-α and ER-β agonists on RAGE expression [50]. In addition, Lata and Mukherjee [51] identified a key role for RAGE in stimulating the proliferation and survival of MCF-7 cells induced by 17α-ethinyl-estradiol, an ER-α agonist. Moreover, in this present study, the location of ER-α (major ER involved in breast cancer development) visualized using confocal fluorescence microscopy showed a massive translocation of ER-α from the cytoplasm to the nucleus after 48 h of treatment with AGEs, with a predominant sequestration into a large nucleolus, site of high transcriptional activity [52]. In addition, in this study, a slight increase of ER-α transcription factor activation in MCF-7 was also

observed after 48 h of treatment with AGEs. ER-α was found sequestrated in multiple small nucleoli at 24- and 72-hour post-treatment with AGEs. Collectively, these results suggest that the MG-BSA-AGEs might contribute to the growth of breast cancer by synergizing with ER-α activation.

With regards to the signaling pathways activated through AGEs/RAGE axis, the phospho-proteome profile of MG-BSA-AGEs-treated MCF-7 cells, luminal breast cancer cell line expressing ER, was far less detectable in contrast to MG-BSA-AGEs-treated MDA-MB-231 cells, basal subtype lacking ER expression, in which increased phosphorylation of p70S6K1, STAT3, p38 MAPK, GSK3 and MKK1/2 were mainly detected, as compared to untreated MDA-MB-231 cells [17]. This difference signaling activation between MCF-7 and MDA-MB-231 cells align with the reported fact that the most aggressive and highly proliferated basal ER-negative sub-type MDA-MB-231 expresses the highest level of RAGE in contrast to the less aggressive luminal ER-positive subtype MCF-7, which showed the lowest level of RAGE expression [53]. In this study using MCF-7 cells, we showed that the MG-BSA-AGEs mainly enhanced the phosphorylation of ERK1/2, MAPK kinase 1/2 (MKK1/2, an activator of phospho-ERK1/2), while MG-BSA-AGEs decreased the phosphorylation of mitogen and stress-activated protein-serine kinase 1 (Msk1, a CREB1 substrate), of different phospho-PKC isoforms (i.e. PKCα, PKCδ and PKCε), and of adducin α (a PKCδ substrate), respectively reported to play a central role in transcription/translation/inflammatory responses/neuronal processes [54], in cell cycle progression/tumorigenesis/metastatic dissemination [55], and in breast cancer progression [56]. Unlike the important kinases implicated in cancer development and progression such as ERK1/2, the phosphorylation of Msk1, which plays a versatile role in transcriptional regulation, and phosphorylation of PKCs have been reported to not necessarily correlate with activation status [51–52]. However, both ERK1/2 and CREB1 are considered as key regulatory proteins in AGEs-promoting cancer including melanogenesis [27]. Furthermore, MG-BSA-AGEs enhance the phosphorylation of ERK1/2 and its upstream activator MKK1/2 in MCF-7 cells at lower levels than those previously detected in MDA-MB-231 cells [17]. The difference in the signaling intensity between the MCF-7 and MDA-MB-231 cells, based on phospho-ERK1/2 overexpression induced by BSA-AGEs, was also seen after chemotherapy with doxorubicin or docetaxel [57]. In addition, MG-BSA-AGEs up-regulated the expression of phospho-CREB1, a transcription factor involved in cell stress responses, cell survival and proliferation. Recently, CREB1, a known ERK2 substrate, has been shown to contribute to breast malignancy by inducing transcription of the aromatase enzyme in breast adipose mesenchymal cells, which leads to increased estrogen levels and, subsequently to cancer development [58–59]. It would therefore be of interest to investigate the impact of MG-BSA-AGEs on the convergence and functional collaboration of ER-α and ERK2 at the genome level that were previously described in MCF-7 cells [60].

In conclusion, we described the stimulatory effects of MG-BSA-AGEs on the proliferation and migration of the hormone-dependent ER-positive breast cancer cell line MCF-7. The investigation of the signaling pathways indicates that MG-BSA-AGEs mainly activate the MAPK pathway and induces the phosphorylation of CREB1 transcription factor in MCF-7 cells; ERK1/2 and CREB1 being widely reported as the main signaling molecules involved in breast cancer development and progression. In addition, MG-BSA-AGEs up-regulate RAGE and ER-α expression through RAGE, suggesting a hypersensitivity of MCF-7 cells to estrogen following to AGEs exposure. Altogether, these findings suggest the need for further studies investigating whether the exposure of AGEs-treated ER-positive breast cancer cells to estrogen could lead to an enhancement of breast cancer development and progression in diabetic patients.

Author contributions

SMN, HS, QW and NA designed the research. HS, SMN, NA, ZR, HA,

WY, NAS, TT and AR conducted the research; SMN, HS, QW, NAS and NA analysed the data and SMN, HS, QW and NA wrote the paper. All authors read and approved the final manuscript.

Competing financial interests

The authors declare no competing financial interests.

Transparency document

The Transparency document associated with this article can be found, in online version.

Acknowledgments

References

[1] L.S. Geiss, J. Wang, Y.J. Cheng, T.J. Thompson, L. Barker, Y. Li, A.L. Albright, E.W. Gregg, Prevalence and incidence trends for diagnosed diabetes among adults aged 20 to 79 years, United States, 1980–2012, JAMA 312 (2014) 1218–1226.

[2] K. Chevreul, K. Berg Brigham, C. Bouché, The burden and treatment of diabetes in France, Glob. Health 10 (2014) 6.

[3] B. Abuyassin, I. Laher, Diabetes epidemic sweeping the Arab world, World J. Diabetes 7 (2016) 165–174.

[4] F. Zaccardi, D.R. Webb, T. Yates, M.J. Davies, Pathophysiology of type 1 and type 2 diabetes mellitus: a 90-year perspective, Postgrad. Med. J. 92 (2016) 63–69.

[5] U. Greifenhagen, A. Frolov, M. Blüher, R. Hoffman, Site-specific analysis of advanced glycation end products in plasma proteins of type 2 diabetes mellitus patients, Anal. Bioanal. Chem. 408 (2016) 5557–5566.

[6] Q. Zhang, J.M. Ames, R.D. Smith, J.W. Baynes, T.O. Metz, A perspective on the Maillard reaction and the analysis of protein glycation by mass spectrometry: probing the pathogenesis of chronic disease, J. Proteome Res. 8 (2009) 754–769.

[7] A.D. McCarthy, A.M. Cortizo, G. Giménez-Segura, L. Bruzzone, S.B. Etcheverry, Non-enzymatic glycosylation of alkaline phosphatase alters its biological properties, Mol. Cell. Biochem. 181 (1998) 63–69.

[8] M. Heilmann, A. Wellner, G. Gadermaier, A. Ilchmann, P. Briza, M. Krause, R. Nagai, S. Burgdof, S. Scheurer, S. Vieths, T. Henle, M. Toda, Ovalbumin modified with pyrraline, a Maillard reaction product, shows enhanced T-cell immunogenicity, J. Biol. Chem. 289 (2014) 7919–7928.

[9] I. Giardino, D. Edelstein, M. Brownlee, Nonenzymatic glycosylation *in vitro* and in bovine endothelial cells alters basic fibroblast growth factor activity. A model for intracellular glycosylation in diabetes, J. Clin. Invest. 94 (1994) 110–117.

[10] G.K. Reddy, Cross-linking in collagen by nonenzymatic glycosylation increases the matrix stiffness in rabbit Achilles tendon, Exp. Diabesity Res. 5 (2004) 143–153.

[11] D. Dobler, N. Ahmed, L. Song, K.E. Eboigbodin, P.J. Thornalley, Increased dicarbonyl metabolism in endothelial cells in hyperglycemia induces anoikis and impairs angiogenesis by RGD and GFOGER motif modification, Diabetes 55 (2006) 1961–1969.

[12] S. Yamagishi, K. Nakamura, H. Inoue, S. Kikuchi, M Takeuchi, Possible participation of advanced glycation end products in the pathogenesis of colorectal cancer in diabetic patients, Med. Hypotheses 64 (2005) 1208–1210.

[13] H.K. Joh, W.C. Willett, E. Cho, Type 2 diabetes and the risk of renal cell cancer in women, Diabetes Care 34 (2011) 1552–1556.

[14] J. Takino, K. Nagamine, T. Hori, A. Sakasai-Sakai, M. Takeuchi, Contribution of the toxic advanced glycation end-products-receptor axis in nonalcoholic steatohepatitis-related hepatocellular carcinoma, World J. Hepatol. 7 (2015) 2459–2469.

[15] C. Gupta, K. Tikoo, High glucose and insulin differentially modulates proliferation in MCF-7 and MDA-MB-231 cells, J. Mol. Endocrinol. 51 (2013) 119–129.

[16] T. Takatani-Nakase, C. Matsui, S. Maeda, S. Kawahara, K. Takahashi, High glucose level promotes migration behavior of breast cancer cells through zinc and its transporters, PLoS One 9 (2014) e90136.

[17] H. Sharaf, S. Matou-Nasri, Q. Wang, Z. Rabhan, H. Al-Eidi, A. Al Abdulrahman, N. Ahmed, Advanced glycation endproducts increase proliferation, migration and invasion of the breast cancer cell line MDA-MB-231, Biochim. Biophys. Acta 1852 (2015) 429–441.

[18] Y. Tang, Y. Wang, M.F. Kiani, B. Wang, Classification, treatment strategy, and associated drug resistance in breast cancer, Clin. Breast Cancer 16 (2016) 353-343.

[19] S. Duss, S. André, A.L. Nicoulaz, M. Fiche, H. Bonnefoi, C. Brisken, R.D. Iggo, An oestrogen-dependent model of breast cancer created by transformation of normal human mammary epithelial cells, Breast Cancer Res. 9 (2007) R38.

[20] M.G. Vander Heiden, L.C. Cantley, C.B. Thompson, Understanding the Warburg effect: the metabolic requirements of cell proliferation, Science 324 (2009) 1029–1033.

[21] F. Hansen, D.F. De Souza, L. Silveira Sda, A.L. Hoefel, J.B. Fontura,

[22] A.C. Tramontina, L.D. Bobermin, M.C. Leite, M.L. Perry, C.A. Gonçalves, Methylglyoxal alters glucose metabolism and increases AGEs content in C6 glioma cells, Metab. Brain Dis. 27 (2012) 531–539.

[22] M.A. Fonseca-Sánchez, S. Rodríguez Cuevas, G. Mendoza-Hernández, V. Bautista-Piña, E. Arechaga Ocampo, A. Hidalgo Miranda, V. Quintanar Jurado, et al., Breast cancer proteomics reveals a positive correlation between glyoxalase 1 expression and high tumor grade, Int. J. Oncol. 41 (2012) 670–680.

[23] C. Ott, K. Jacobs, E. Haucke, A. Navarrete Santos, T. Grune, A. Simm, Role of advanced glycation end products in cellular signaling, Redox Biol. 9 (2014) 411–429.

[24] R. López-Díez, A. Rastrojo, O. Villate, B. Aguado, Complex tissue-specific patterns and distribution of multiple RAGE splice variants in different mammals, Genome Biol. Evol. 5 (2013) 2420–2435.

[25] D. Yao, M. Brownlee, Hyperglycemia-induced reactive oxygen species increase expression of the receptor for advanced glycation end products (RAGE) and RAGE ligands, Diabetes 59 (2010) 249–255.

[26] R.G. Iannitti, A. Casagrande, A. De Lucas, C. Cunha, G. Sorci, F. Riuzzi, M. Borghi, et al., Hypoxia promotes danger-mediated inflammation via receptor for advanced glycation end products in cystic fibrosis, Am. J. Respir. Crit. Care Med. 188 (2013) 1338–1350.

[27] E.J. Lee, J.Y. Kim, S.H. Oh, Advanced glycation end products (AGEs) promote melanogenesis through receptor for AGEs, Sci Rep 6 (2016) 27848.

[28] S. Liao, J. Li, W. Wei, L. Wang, Y. Zhang, J. Li, C. Wang, S. Sun, Association between diabetes mellitus and breast cancer risk: a meta-analysis of the literature, Asian Pac. J. Cancer Prev. 12 (2011) 1061–1065.

[29] C.C. Lin, J.H. Chiang, C.I. Li, C.S. Liu, W.Y. Lin, T.F. Hsieh, T.C. Li, Cancer risks among patients with type 2 diabetes: a 10-year follow-up study of a nationwide population-based cohort in Taiwan, BMC Cancer 14 (2014) 381.

[30] Z. Suba, Circulatory estrogen level patients against breast cancer in obese women, Recent Pat. Anticancer Drug Discov. 8 (2013) 154–167.

[31] A.A. Onitilo, R.V. Stankowski, R.L. Berg, J.M. Engel, I. Glurich, G.M. Williams, S.A. Doi, Type 2 diabetes mellitus, glycemic control, and cancer risk, Eur. J. Cancer Prev. 23 (2014) 134–140.

[32] K.B. Michels, C.G. Solomon, F.B. Hu, B.A. Rosner, S.E. Hankinson, G.A. Colditz, J.E. Manson, Nurses' health study, Type 2 diabetes and subsequent incidence of breast cancer in the Nurses' health study, Diabetes Care 26 (2003) (1752-1758).

[33] E. Ziegler, M.T. Hansen, M. Haase, G. Emons, C. Gründker, Generation of MCF-7 cells with aggressive metastatic potential *in vitro* and *in vivo*, Breast Cancer Res. Treat. 148 (2014) 269–277.

[34] H. Frankowski, Y.H. Gu, J.H. Heo, G.J. del Zoppo, Use of gel zymography to examine matrix metalloproteinase (gelatinase) expression in brain tissue or in primary glial cultures, Methods Mol. Biol. 814 (2012) 221–233.

[35] A.J. Urtreger, M.G. Kazanietz, E.D. Bal de Kier Joffé, Contribution of individual PKC isoforms to breast cancer progression, IUBMB Life 64 (2012) 18–26.

[36] M.W. Nasser, N.A. Wani, D.K. Ahirwar, C.A. Powell, J. Ravi, M. Elbaz, H. Zhao, et al., RAGE mediates S100A7-induced breast cancer growth and metastasis by modulating the tumor microenvironment, Cancer Res. 75 (2015) 974–985.

[37] A.M. Scherbakov, D.V. Sorokin, V.V. Jr Tatarskiy, N.S. Prokhorov, S.E. Semina, L.M. Berstein, M.A. Krasil'nikov, The phenomenon of acquired resistance to metformin in breast cancer cells: the interaction of growth pathways and estrogen receptor signaling, IUBMB Life 68 (2016) 281–292.

[38] D.J. Lobbezoo, R.J. van Kampen, A.C. Voogd, M.W. Dercksen, F. van den Berkmortel, T.J. Smilde, A.J. van de Wouw, et al., Prognosis of metastatic breast cancer subtypes: the hormone receptor/HER2-positive subtype is associated with the most favorable outcome, Breast Cancer Res. Treat. 141 (2013) 507–514.

[39] R.G. Posner, J. Bold, Y. Bernstein, J. Rasor, J. Braslow, W.S. Hlavacek, A.S. Perelson, Measurement of receptor crosslinking at the cell surface via multi-parameter flow cytometry, Proc. SPIE 3256 Advances in Optical Biophysics, 3256 1998, pp. 132–143.

[40] D. Xu, J.H. Young, J.M. Krahn, D. Song, K.D. Corbett, W.J. Chazin, L.C. Pedersen, J.D. Esko, Stable RAGE-heparan sulfate complexes are essential for signal transduction, ACS Chem. Biol. 8 (2013) 1611–1620.

[41] K.C. Lan, C.Y. Chiu, C.W. Kao, K.H. Huang, C.C. Wang, K.T. Huang, K.S. Tsai, et al., Advanced glycation end-products induce apoptosis in pancreatic islet endothelial cells via NF-kB-activated cyclooxygenase-2/prostaglandin E2 up-regulation, PLoS One 11 (2015) e0124418.

[42] A. Dufour, N.S. Sampson, S. Zucker, J. Cao, Role of the hemopexin domain of matrix metalloproteinases in cell migration, J. Cell. Physiol. 217 (2008) 643–651.

[43] N. Sevillano, M.D. Girón, M. Salido, A.M. Vargas, J. Vilches, R. Salto, Internalization of the receptor for advanced glycation end products (RAGE) is required to mediate intracellular responses, J. Biochem. 145 (2009) 21–30.

[44] N. Tanaka, H. Yonekura, S. Yamagishi, H. Fujimori, Y. Yamamoto, H. Yamamoto, The receptor for advanced glycation end products is induced by the glycation products themselves and tumor necrosis factor-alpha through nuclear factor-kappa B, and by 17 beta-estradiol through Sp-1 in human vascular endothelial cells, J. Biol. Chem. 275 (2000) 25781–25790.

[45] A. Ström, J. Hartman, J.S. Foster, S. Kietz, J. Wimalasena, J.A. Gustafsson, Estrogen receptor beta inhibits 17 beta-estradiol-stimulated proliferation of the breast cancer cell line T47D, Proc. Natl. Acad. Sci. U. S. A. 101 (2004) 1566–1571.

[46] C. Zhao, J. Matthews, M. Tujaque, J. Wan, A. Ström, G. Toresson, E.W. Lam, et al., Estrogen receptor beta2 negatively regulates the transactivation of estrogen receptor alpha in human breast cancer cells, Cancer Res. 67 (2007) 3955–3962.

[47] A. Rody, U. Holtrich, C. Solbach, K. Kourtis, G. von Minckwitz, K. Engels, S. Kissler, et al., Methylation of estrogen receptor beta promoter correlates with loss of ER-beta expression in mammary carcinoma and is an early indication marker in premalignant lesions, Endocr. Relat. Cancer 12 (2005) 903–916.

[48] A. El-Osta, D. Brasacchio, D. Yao, A. Pocai, P.L. Jones, R.G. Roeder, M.E. Cooper,

M. Brownlee, Transient high glucose causes pertinent epigenetic changes and altered gene expression during subsequent normoglycemia, J. Exp. Med. 205 (2008) 2409–2417.

[49] H. Al-Nakhle, P.A. Burns, M. Cummings, A.M. Hanby, T.A. Hughes, S. Satheesha, A.M. Shaaban, L. Smith, V. Speirs, Estrogen receptor-β1 expression is regulated by miR-92 in breast cancer, Cancer Res. 70 (2010) 4778–4784.

[50] T.K. Mukherjee, P.R. Reynolds, J.R. Hoidal, Differential effect of estrogen receptor alpha and beta agonists on the receptor for advanced glycation end product expression in human microvascular endothelial cells, Biochim. Biophys. Acta 1745 (2005) 300–309.

[51] K. Lata, T.K. Mukherjee, Knockdown of receptor for advanced glycation end products attenuate 17α-ethinyl-estradiol dependent proliferation and survival of MCF-7 breast cancer cells, Biochim. Biophys. Acta 1840 (2014) 1083–1091.

[52] M. Carraz, W. Zwart, T. Phan, R. Michalides, L. Brunsveld, Perturbation of receptor α localization with synthetic nona-arginine LXXLL-peptide coactivator binding inhibitors, Chem. Biol. 16 (2009) 702–711.

[53] A.M. Radia, A.M. Yaser, X. Ma, J. Zhang, C. Yang, Q. Dong, P. Rong, B. Ye, S. Liu, W. Wang, Specific siRNA targeting receptor for advanced glycation endproducts (RAGE) decreases proliferation in human breast cancer cell lines, Int. J. Mol. Sci. 14 (2013) 7959–7978.

[54] L. Vermeulen, W. Vanden Berghe, I.M. Beck, K. De Bosscher, G. Haegeman, The versatile role of MSKs in transcriptional regulation, Trends Biochem. Sci. 34 (2009) 311–318.

[55] R. Garg, L.G. Benedett, M.B. Abera, H. Wang, M. Abba, M.G. Kazanietz, Protein kinase C and cancer: what we know and what we do not, Oncogene 33 (2014) 5225–5237.

[56] S.C. Kiley, K.J. Clark, S.K. Duddy, D.R. Welch, S. Jaken, Increased protein kinase Cδ in mammary tumor cells: relationship to transformation and metastatic progression, Oncogene 18 (1999) 6748–6757.

[57] A. Taherian, T. Mazoochi, Different expression of extracellular signal-regulated kinase (Erk) 1/2 and phospho-Erk proteins in MDA-MB-231 and MCF-7 cells after chemotherapy with doxorubicin or docetaxel, Iran J. Basic Med. Sci. 15 (2012) 669–677.

[58] A. Chhabra, H. Fernando, G. Watkins, R.E. Mansel, W.G. Jiang, Expression of transcription factor CREB1 in human breast cancer and its correlation with prognosis, Oncol. Rep. 18 (2007) 953–958.

[59] N.U. Samarajeewa, M.M. Docanto, E.R. Simpson, K.A. Brown, CREB-regulated transcription co-activator family stimulates promoter II-driven aromatase expression in preadipocytes, Horm. Cancer 4 (2013) 233–241.

[60] Z. Madak-Erdogan, M. Lupien, F. Stossi, M. Brown, B.S. Katzenellenbogen, Genomic collaboration of estrogen receptor α and extracellular signal-regulated kinase 2 in regulating gene and proliferation programs, Mol. Cell. Biol. 31 (2011) 226–236.